Extended X-Ray Absorption Fine Structure Study of Local Structure and Atomic Correlations of Tellurium Nanoparticles

Hiroyuki Ikemoto*
Department of Physics, University of Toyama, Toyama 930-8555, Japan

Takafumi Miyanaga
Department of Advanced Physics, Hirosaki University, Hirosaki 036-8561, Japan
(Received 15 May 2007; published 18 October 2007)

Extended x-ray absorption fine structure measurements were performed on trigonal tellurium (*t*-Te) and tellurium nanoparticles in very thin films. Twofold coordinated chains, much like those in *t*-Te, exist even in the nanoparticles, but covalent bonds or intrachain interactions are stronger than those of *t*-Te as shown by a shorter bond length and higher Einstein temperature. The interchain coordination number of the nanoparticles is about half that of *t*-Te, suggesting reduction of interchain interactions.

DOI: 10.1103/PhysRevLett.99.165503 PACS numbers: 61.46.Df, 33.15.Dj, 36.20.Fz, 61.10.Ht

The number of atoms constituting individual particles plays an important role in determining the physical properties and structure of a material. The surface effect is an important factor, particularly for nm-size particles [1]. In typical semiconductor materials such as germanium, the surface is known to have a different structure from that of the bulk [2]. To date, the structure and physical properties of small particles have mostly been studied for metals and semiconductor materials (Si, Ge, CdS, and so on) [3,4]. In comparison, the number of studies carried out on materials with an exotic structure, that is, materials having a secondary structure, is small.

As in the case of selenium, trigonal tellurium (*t*-Te) has a highly anisotropic crystal structure consisting of helical chains of covalently bound atoms with three atoms per turn, which are in turn bound together into a hexagonal lattice ($a = 4.456$ Å, $c = 5.921$ Å) [5]. The hybridization between the lone-pair (LP) orbitals and the antibonding orbitals in the adjacent chain brings about interchain interactions, and the distance to the interchain nearest neighbor is smaller than twice the van der Waals radius. Tellurium exists only in the trigonal form, while selenium also forms monoclinic variants where the basic unit is a crownlike Se_8 ring. The chalcogen chains are flexible, so there is a possibility that Te nanoparticles have exotic structures; that is, the chains are folded and tangled up like yarn, or the surface effects are negligible in the Te nanoparticles.

Extended x-ray absorption fine structure (EXAFS) analysis is a powerful tool for studying the local coordination and dynamics of selected atomic species in condensed matter [6]. A prominent feature of the EXAFS analysis is that it makes no difference whether a crystalline or disordered material is being studied in terms of the quality of the obtainable structural parameters. The EXAFS function $\chi(k)$ can be expressed by a cumulant expansion for the structural and thermal disorders. The first three cumulants correspond to the average value, the variance, and the asymmetry of the distance distribution for a given coordination shell. Temperature variations of the second-order cumulant (Debye-Waller factor, σ^2) and third-order cumulant (C_3) give information on the thermal disorder, and anharmonicity of the interatomic potential, respectively. Here, we report the local structure of the Te nanoparticles obtained by EXAFS measurements.

Tellurium of 99.999% purity was slowly deposited onto substrates from an alumina crucible. The formed Te film was discontinuous with isolated island formation. Then, NaCl of 99.99% purity was deposited to cover the Te islands. By repeating these steps, samples of the Te nanoparticles isolated in a NaCl matrix were obtained [7]. The thickness was monitored with a quartz oscillator, and the ratio of the thickness of Te to that of NaCl was 1:20. As mentioned above, the Te nanoparticles were formed in thin films, and, in this Letter, samples are referred to by their average Te thin film thickness. To confirm the formation of nanoparticles, 10-nm-thick films were observed by field emission scanning electron microscopy (FESEM) (JEOL JSM-6700F at the Center for Instrumental Analysis, University of Toyama). The diameter of the nanoparticles was determined to be 66 ± 17 nm. It is indisputable that the nanoparticles were formed in the 0.5-nm-thick films, but we have not yet observed them directly due to technical difficulties at this stage.

X-ray absorption measurements were performed using the spectrometer installed at NW10A of the Photon Factory (PF-AR) in the High Energy Accelerator Research Organization (KEK), Tsukuba, Japan. EXAFS data were obtained for the Te *K*-edge (31.8 keV). The intensities of the incident beam and the transmitted beam were monitored by ionization chambers.

The Fourier transform (FT) of $k\chi(k)$ data provides useful information for identifying atomic correlations. The experimentally obtained EXAFS signals were Fourier-transformed with a Hamming window in the range from

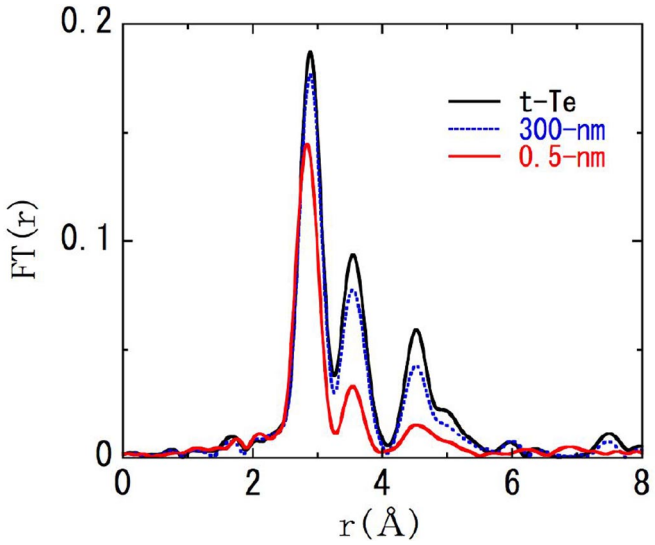

FIG. 1 (color online). Fourier transform magnitude of EXAFS $k\chi(k)$ data measured at 20 K for t-Te, 300-nm-thick films, and 0.5-nm-thick films.

4 to 18 Å^{-1}. FTs at 20 K for t-Te, the 300- and 0.5-nm-thick films are presented in Fig. 1. There are three prominent peaks at 2.88, 3.54, and 4.53 Å for t-Te. By comparison with x-ray diffraction measurements (XRD) in the literature [5], the first and second peaks are assigned to contributions from the intrachain first nearest neighbor (1NN) and the interchain 1NN distances, respectively. The third peak corresponds to the second nearest neighbor (2NN) distances of the intra- and interchain, that is, 4.4408 and 4.4560 Å [5], respectively.

The first and second peaks overlap each other, but are well separated from the third peak. The Fourier peaks were filtered in the range of 2.5 and 4.0 Å for t-Te, inverse Fourier transformed into k-space again and divided by the same Hamming window function in order to extract the peaks originating from the intra- and interchain 1NNs. The EXAFS function, $k^2\chi(k)$, for t-Te was fitted by a nonlinear least-squares method to the theoretical function within the frame of a two-shell model with Te-Te atomic pairs and up to C_3 [8]. The phase shift, backscattering amplitude, and electron mean free path were calculated using the FEFF8.4 code [9]. The amplitude reduction factor was chosen to make the average of the 1NN coordination number N_1 below 100 K for t-Te equal to 2.00. At temperatures higher than 100 K, N_1 decreases slightly and reaches 1.91 at 300 K. However, it makes no physical sense that N_1 decreases within the range of measurement temperatures, and the quality of EXAFS signals at temperatures higher than 100 K is inferior. The difference in 1NN distance r_1 between 20 and 300 K is 0.0017 Å, which is sufficiently below the resolution of the EXAFS analysis. The average of 1NN C_3 for all measurement temperatures is $8.37 \pm 44(\times 10^{-6}$ Å$^3)$. The parameters for intrachain 1NN, r_1, N_1, and C_3 do not show any temperature dependence and are constant in the present temperature range. So the values are averaged below 100 K. Structural parameters obtained from the fit to the experimental spectra for the intra- and interchain 1NN atoms are shown in Table I. The uncertainties on structural parameters are estimated from the standard deviations of the experimental data below 100 K. The obtained r_1 of t-Te and the 300-nm-thick films are in complete accordance with the literature [5] without any constraints for the atomic distances.

In the analysis of the 0.5-nm-thick films, the same two-shell curve fitting as for t-Te was performed. Although only the Te-Te shells were assumed, residual errors (R-factor in Table I) of the 0.5-nm-thick films are comparable with those of t-Te and the 300-nm-thick films. In addition, C_3 of the intrachain 1NN is negligibly small taking into account the fact that the standard values are of the order of 10^{-4} Å^3, which reveals that the potential for the intrachain 1NN is symmetric. These results may imply that the obtained EXAFS signals for the 0.5-nm-thick films result from the single-species Te chains of the nanoparticles. At the very least, halides, oxides, and so on are not present, which means that the Te atoms do not form any chemical bonding with other elements.

The most striking features of the 0.5-nm-thick films are shrinkage and preservation of the coordination number of the covalent bonds within the chains. The bond distance is 0.042 Å shorter than that of t-Te and the 300-nm-thick films, corresponding to strengthening of the covalent bonds. In the FT spectra, the third peak of the 0.5-nm-thick films is located at the same distance as that of t-Te. As stated above, the peak contains the intra- and interchain 2NN peaks, and it can be guessed that the intrachain 2NN distance is similar to that of t-Te. This suggests that bond angle is similar to that of t-Te. The twofold coordinated

TABLE I. Structural parameters obtained from the best fit to the EXAFS experimental spectra for t-Te, the 300- and the 0.5-nm-thick films. Statistical calculations were performed below 100 K.

	Intrachain			Interchain	
	r_1 [Å]	N_1	$C_3 \times 10^{-6}$ [Å^3]	N_2	R-factor
t-Te [5]	2.835	2.00		4.00	
t-Te	2.834 ± 0.002	2.00 ± 0.05	−23 ± 46	4.25 ± 0.30	9.9
300-nm	2.837 ± 0.004	1.99 ± 0.15	45 ± 50	4.47 ± 0.18	10.9
0.5-nm	2.792 ± 0.001	1.94 ± 0.03	20 ± 22	2.17 ± 0.31	10.5

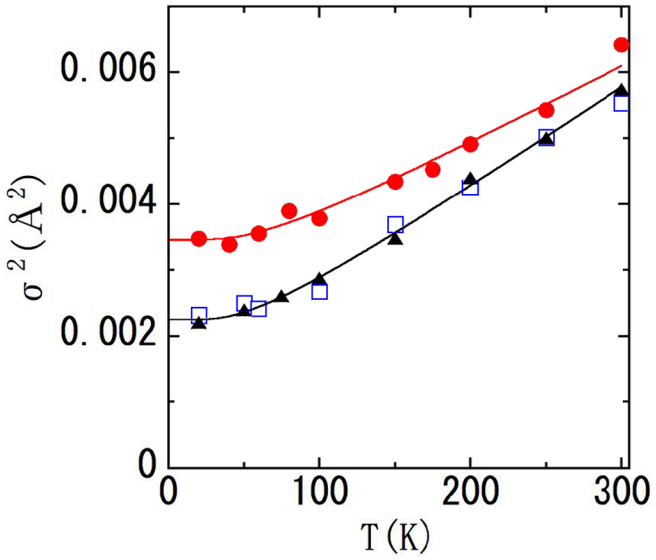

FIG. 2 (color online). Debye-Waller factor σ_1^2 of the nearest neighbor within chains for several Te systems as a function of the measurement temperature, with the respective correlated Einstein model fits for *t*-Te and the 0.5-nm-thick films (lines). The triangles denote σ_1^2 for *t*-Te; the squares denote σ_1^2 for the 300-nm-thick films; the circles denote σ_1^2 for the 0.5-nm-thick films.

chain structure specific to *t*-Te is preserved even in the 0.5-nm-thick films, but the covalent bond is shorter and stronger than that of *t*-Te.

The Debye-Waller factor σ_1^2 for the intrachain 1NN is shown as a function of the measurement temperature in Fig. 2. The lines denote fits obtained with the correlated Einstein models for *t*-Te and the 0.5-nm-thick films. The values obtained from such fits for the static contribution (σ_S^2) and for the thermal one (given in terms of the Einstein temperature Θ_E) to the total disorder are shown in Table II.

At all temperatures, values of σ_1^2 of the 0.5-nm-thick films are larger than those of *t*-Te and the 300-nm-thick films. But the thermal evolution of σ_1^2 of the former is slower than those of the others, as can be observed by the smaller slope of the curve best fitting the data. The value of Θ_{E_1} of the 0.5-nm-thick films is higher than those of the others, also suggesting a hardening of covalent bonding in the 0.5-nm-thick films.

The average coordination numbers (N_2) for the interchain 1NN below 100 K are listed in Table I. Those for *t*-Te and the 300-nm-thick films are about 10% larger than the real coordination number of 4.00. Though we cannot explain this slightly strange result at this stage, possible explanations may be the overlap between the intra- and interchain peaks and the weak intensity of the interchain correlation. Despite this discrepancy, there is a marked difference between the 0.5-nm-thick films and the others, that is, N_2 of the 0.5-nm-thick films is about half that of the others. This indicates that the interchain interactions are reduced in the 0.5-nm-thick films.

The interatomic distances r_2 for the interchain 1NN are shown in Fig. 3 as functions of temperature. A solid line denotes the values of r_2 calculated with coefficients of linear expansion [10] and the literature value of r_2 at room temperature [5]. The values of r_2 obtained from EXAFS measurements are about 0.015 Å larger than those calculated with the literature values, but their temperature dependences are similar. This difference may originate from the same reason due to the overlapping of the two peaks as N_2 is larger than 4. At 20 K, the value of r_2 of the 0.5-nm-thick films is close to those of *t*-Te and the 300-nm-thick films. The temperature variations of r_2 of the 0.5-nm-thick films are very large compared with those of the others, implying that the interchain interactions of the 0.5-nm-thick films are weaker than those of the others.

If the Einstein frequency or Einstein temperature Θ_E can be estimated by harmonic oscillator approximation, Θ_E of *t*-Te would be obtained as 135 and 61 K by using the force constants [11] for the intrachain and interchain 1NN distances, respectively. In spite of this bold assumption, values of Θ_E calculated with the force constants (135 and 61 K) are consistent in principle with those obtained from EXAFS measurements (156.9 and 83.3 K) for *t*-Te. If the relation between Θ_E and the force constant is reliable, the force constant for the intrachain interactions of the 0.5-nm-thick films is 1.3 times stronger than that of *t*-Te. There is an empirical relation between the covalent bond length and the force constant [12]. The force constant for the intrachain interactions of the 0.5-nm-thick films estimated from the bond distances (r_1 in Table I) is about 1.1 times stronger than that of *t*-Te, which is similar to that obtained from the present Θ_E, in spite of the bold assumption.

A stable form of selenium, which is a congener of Te, is trigonal, similar to Te. Isolated Se chains encapsulated within mordenite, which has one-dimensional channels with a diameter of 6.7 Å, have been studied. Due to the

TABLE II. Einstein temperatures and static components of the Debye-Waller factors obtained from best fits of the correlated Einstein model to the experimentally obtained temperature-dependent data.

	Intrachain		Interchain	
	Θ_{E_1} [K]	$\sigma_{S_1}^2$ [Å^2]	Θ_{E_2} [K]	$\sigma_{S_2}^2$ [Å^2]
t-Te	156.9	0.0010	83.3	0.0032
300-nm	162.2	0.0012	81.7	0.0037
0.5-nm	178.0	0.0024	79.1	0.0053

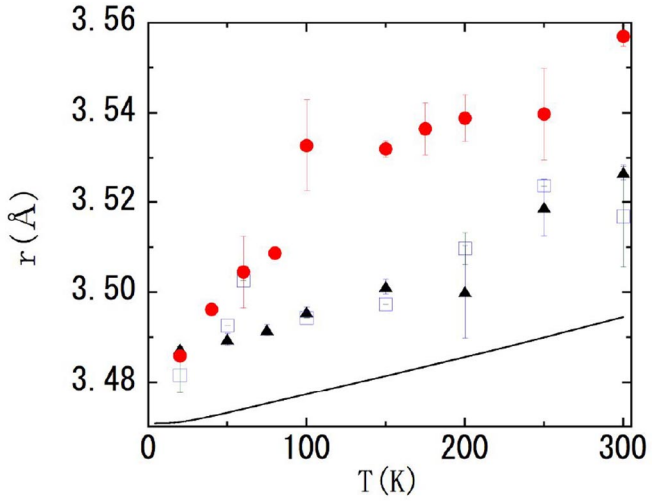

FIG. 3 (color online). Thermal evolution of interatomic distance r_2 of the interchain 1NN for t-Te, the 0.5 and 300-nm-thick films. The triangles represent r_2 for t-Te; the squares represent r_2 for the 300-nm-thick films; the circles represent r_2 for the 0.5-nm-thick films. The solid line denotes the values calculated with literature values.

confinement, the value of r_1 reduces to 2.34 from 2.37 Å of t-Se [13], and the Raman frequency assigned to the symmetric bond-stretching mode of the chain increases [14]. This can be explained as follows: removal of the interchain interactions induces shrinkage and enhancement of bonding of the intrachain 1NN because the hybridization between the LP and the antibonding on adjacent chains weakens the intrachain covalent bond. The same scenario can be adopted for the Te nanoparticles. The covalent bond shrinkage and the enhancement of the force constant for the 0.5-nm-thick films are induced by the reduction of the interchain interactions, which is encouraged by the decrease of N_2.

In summary, important characteristics determined for Te nanoparticles of 0.5-nm-thick films are as follows: the existence of a covalently bonded chain structure; shrinkage of the bonds; an increase in the force constant for the intrachain 1NN; and a decrease in interchain interactions. The twofold coordinated covalent bonds are similar to those of t-Te and the chain structure is preserved, whereas the interchain interactions are easily reduced because the interchain interactions are weaker than the intrachain interactions. The decrease in the overlap between the orbitals in adjacent chains, together with weakening of the interchain interactions, gives rise to the covalent bond shrinkage. The decrease also suggests that the chains are arranged randomly in the Te nanoparticles, that is, the nanoparticles should be amorphous in consideration that the overlap between the orbitals in adjacent chains brings order between chains in t-Te.

The authors would like to thank Mr. S. Yoshida, A. Goyo, and K. Nitta for their assistance at various stages. The synchrotron radiation experiments were performed at the Photon Factory in KEK under Proposal No. 2005G193.

*ikemoto@sci.u-toyama.ac.jp

[1] P. Zhang and T. K. Sham, Phys. Rev. Lett. **90**, 245502 (2003).
[2] M. Mitome and K. Takayanagi, Ultramicroscopy **39**, 382 (1991).
[3] C. Burda, X. Chen, R. Narayanan, and M. A. El-Sayed, Chem. Rev. **105**, 1025 (2005).
[4] T. Trindade and P. O'Brien, N. L. Pickett, Chem. Mater. **13**, 3843 (2001).
[5] C. Adenis, V. Langer, and O. Lindqvist, Acta Crystallogr. Sect. C **45**, 941 (1989).
[6] *X-ray Absorption*, edited by D. C. Koningsberger and R. Prins (Wiley, New York, 1988).
[7] T. Tsuzuki, M. Yao, and H. Endo, J. Phys. Soc. Jpn. **64**, 485 (1995).
[8] H. Endo, K. Maruyama, H. Hoshino, and H. Ikemoto, Z. Phys. Chem. (Frankfort/Main) **217**, 863 (2003).
[9] A. L. Ankudinov, B. Ravel, J. J. Rehr, and S. D. Conradson, Phys. Rev. B **58**, 7565 (1998).
[10] M. Hortal and A. J. Leadbetter, J. Phys. C **5**, 2129 (1972).
[11] H. Wendel, J. Phys. C **9**, 445 (1976).
[12] G. R. Freeman and N. H. March, J. Mol. Struct. (Theochem) **333**, 261 (1995).
[13] M. Inui, M. Yao, and H. Endo, J. Phys. Soc. Jpn. **57**, 553 (1988).
[14] V. V. Poborchii, A. V. Kolobov, H. Oyanagi, S. G. Romanov, and K. Tanaka, Chem. Phys. Lett. **280**, 10 (1997).